Electronic Supporting Information

Dibenzotetraaza[14]annulene – adenine conjugate recognizes complementary poly dT among ss-DNA / ss-RNA sequences

Marijana Radić Stojković,[a] Marko Škugor,[a] Sanja Tomić,[a] Marina Grabar,[a] Vilko Smrečki,[a] Łukasz Dudek,[b] Jarosław Grolik,[b] Julita Eilmes[b] and Ivo Piantanida*[a]

[a] Division of Organic Chemistry and Biochemistry, Division of Physical Chemistry, NMR Centre, Ruđer Bošković Institute, Bijenička cesta 54, PO Box 180, HR-10002 Zagreb, Croatia, E-mail: pianta@irb.hr
[b] Department of Chemistry, Jagiellonian University, Ingardena 3 ,30-060 Kraków, Poland

SUPPORTING INFORMATION

Contents

1 Additional characterisation data for compounds 1-3:

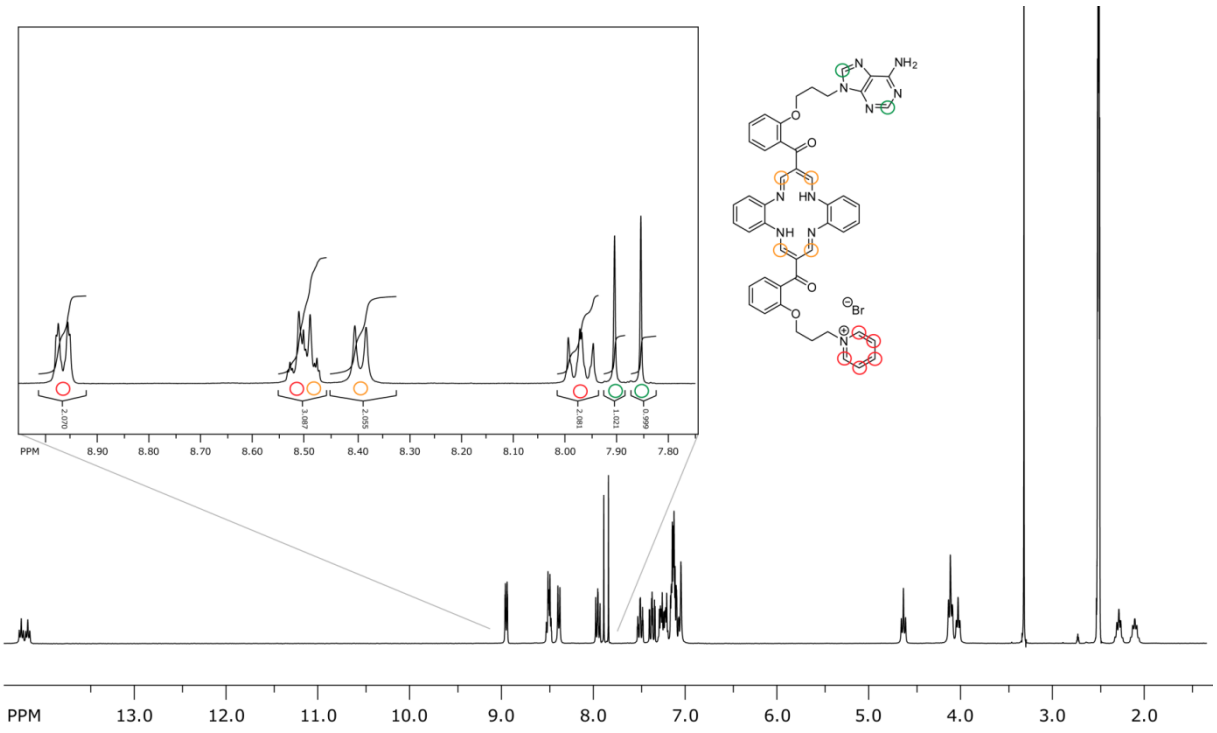

^{1}H-NMR spectrum of **1** in DMSO-d_6

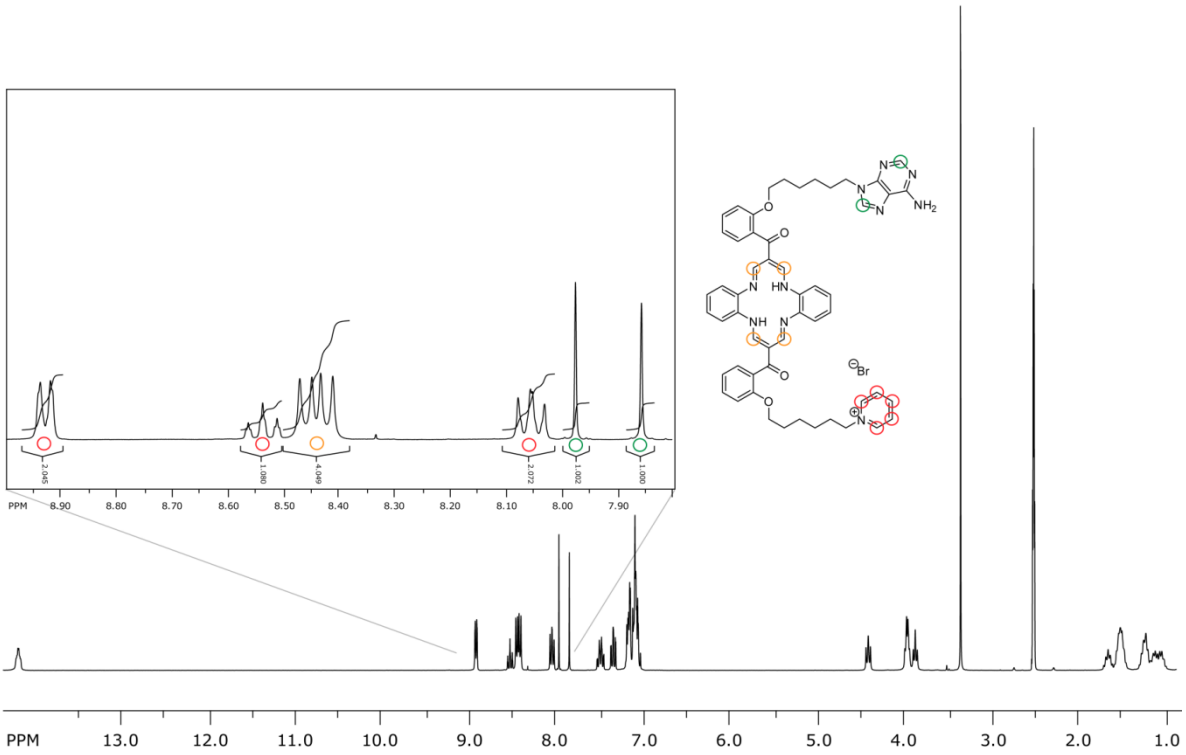

^{1}H-NMR spectrum of **2** in DMSO-d_6

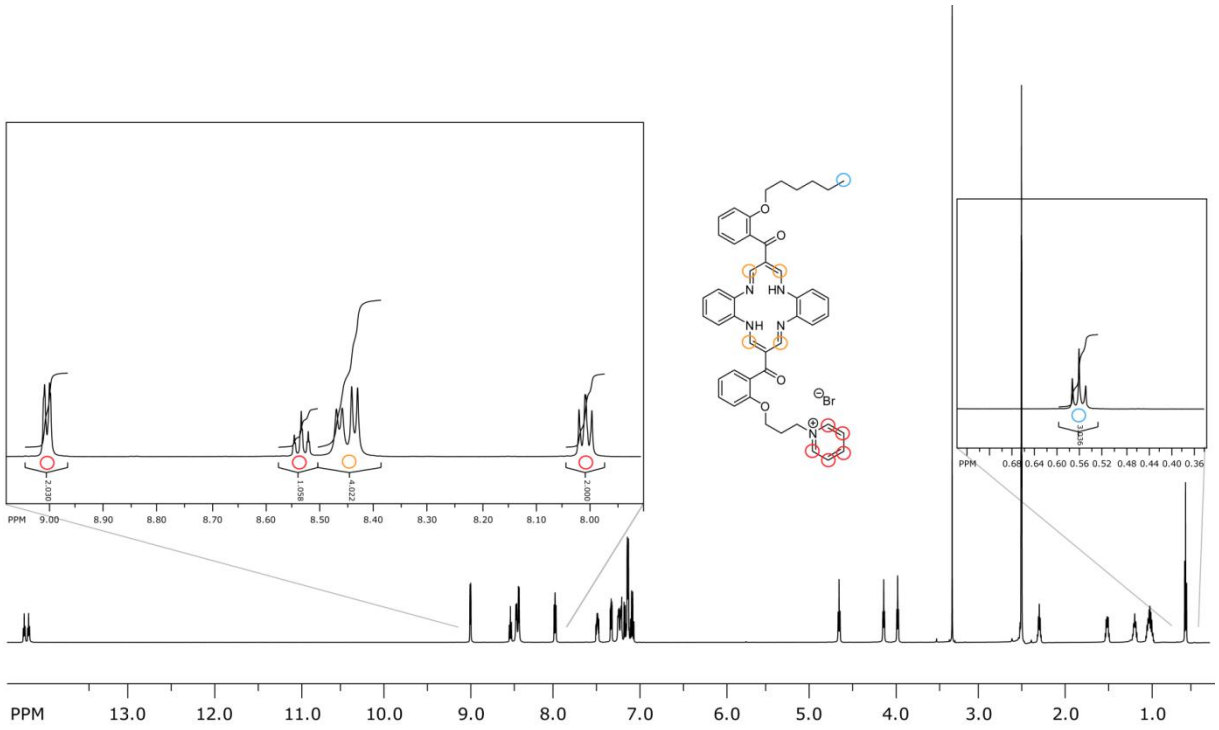

^{1}H-NMR spectrum of **3** in DMSO-d_6

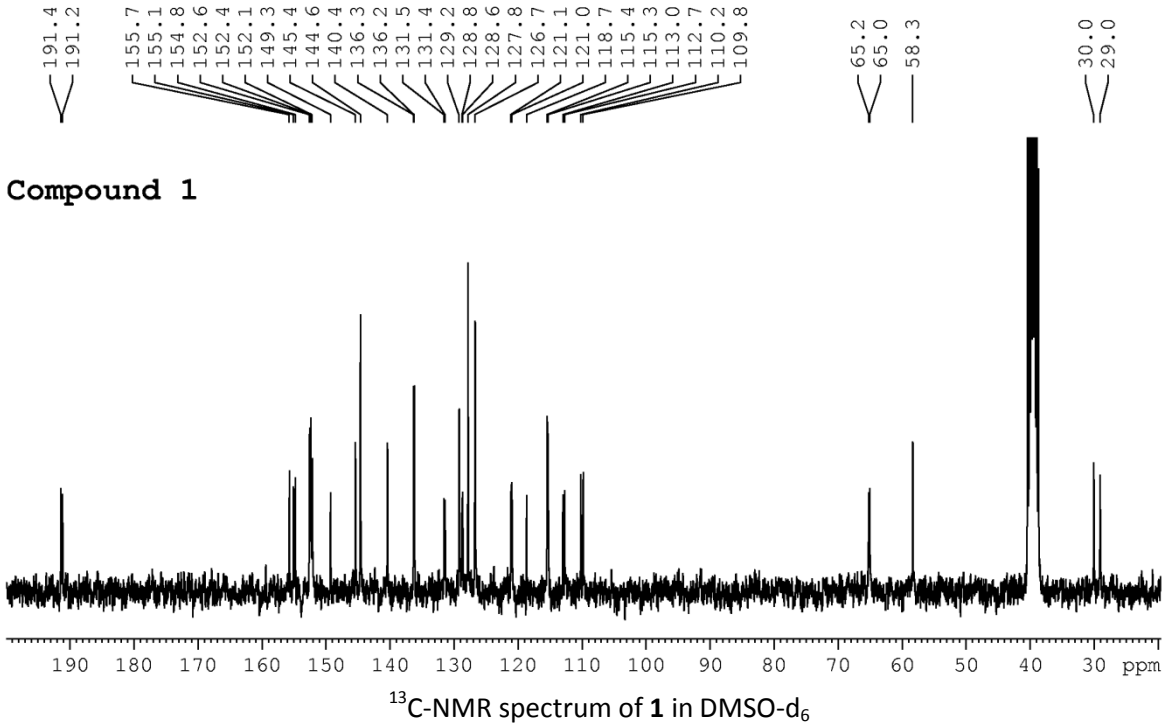

^{13}C-NMR spectrum of **1** in DMSO-d_6

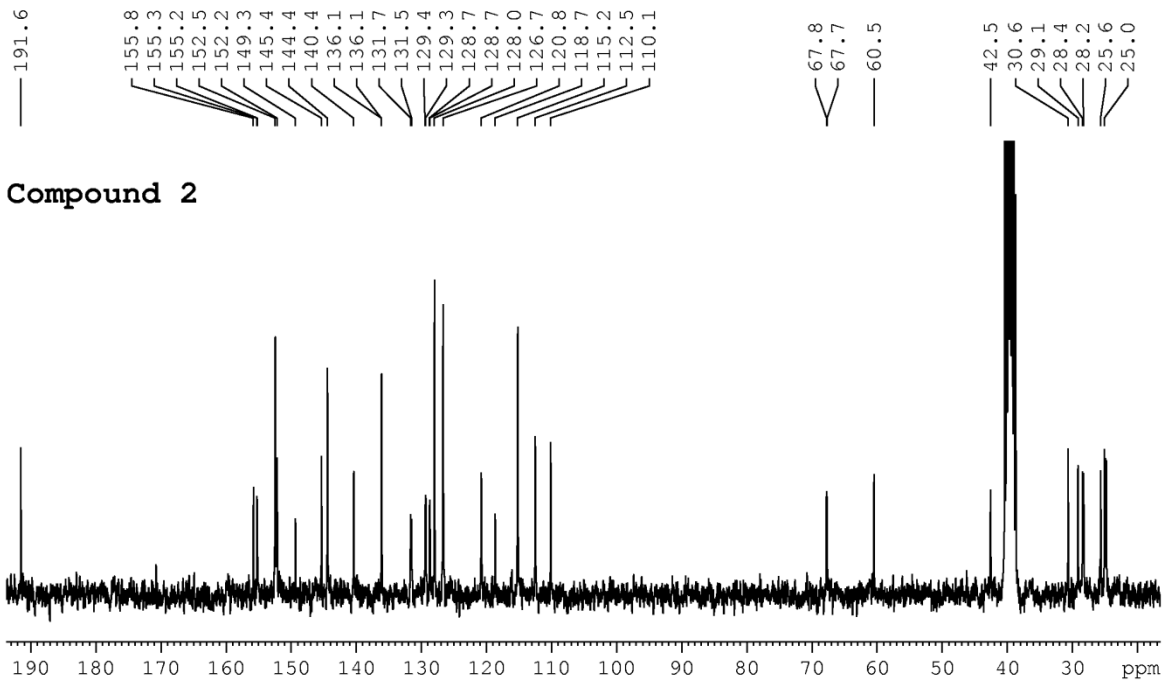

^{13}C-NMR spectrum of **2** in DMSO-d_6

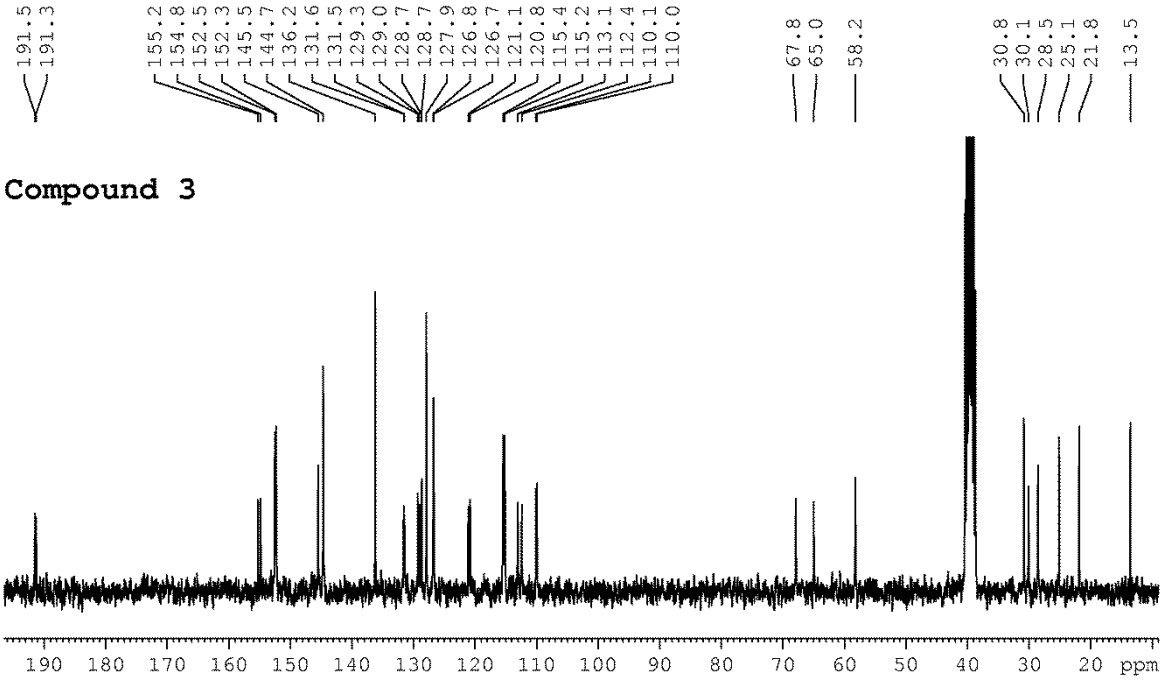

^{13}C-NMR spectrum of **3** in DMSO-d_6

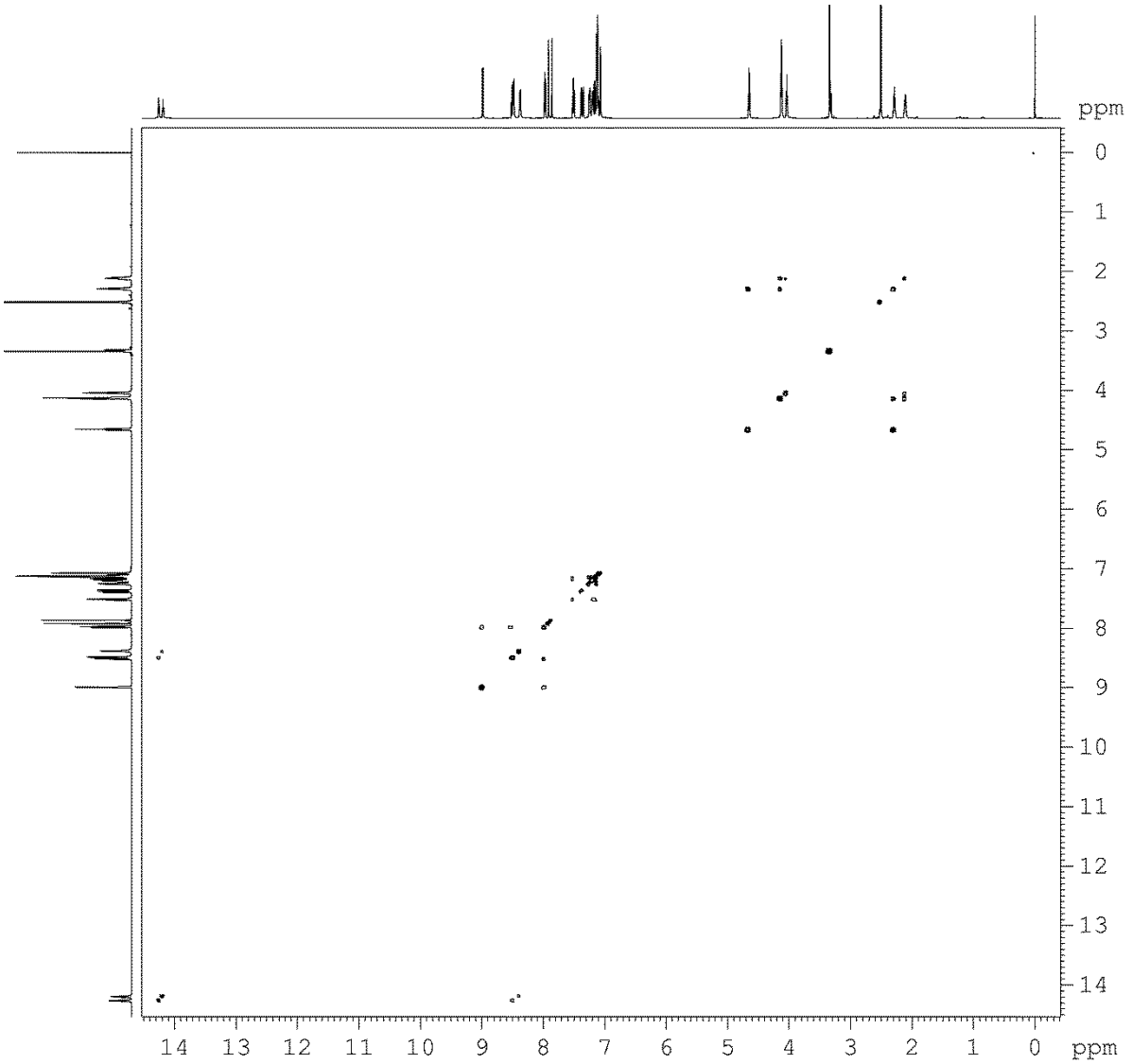

COSY spectrum of **1**

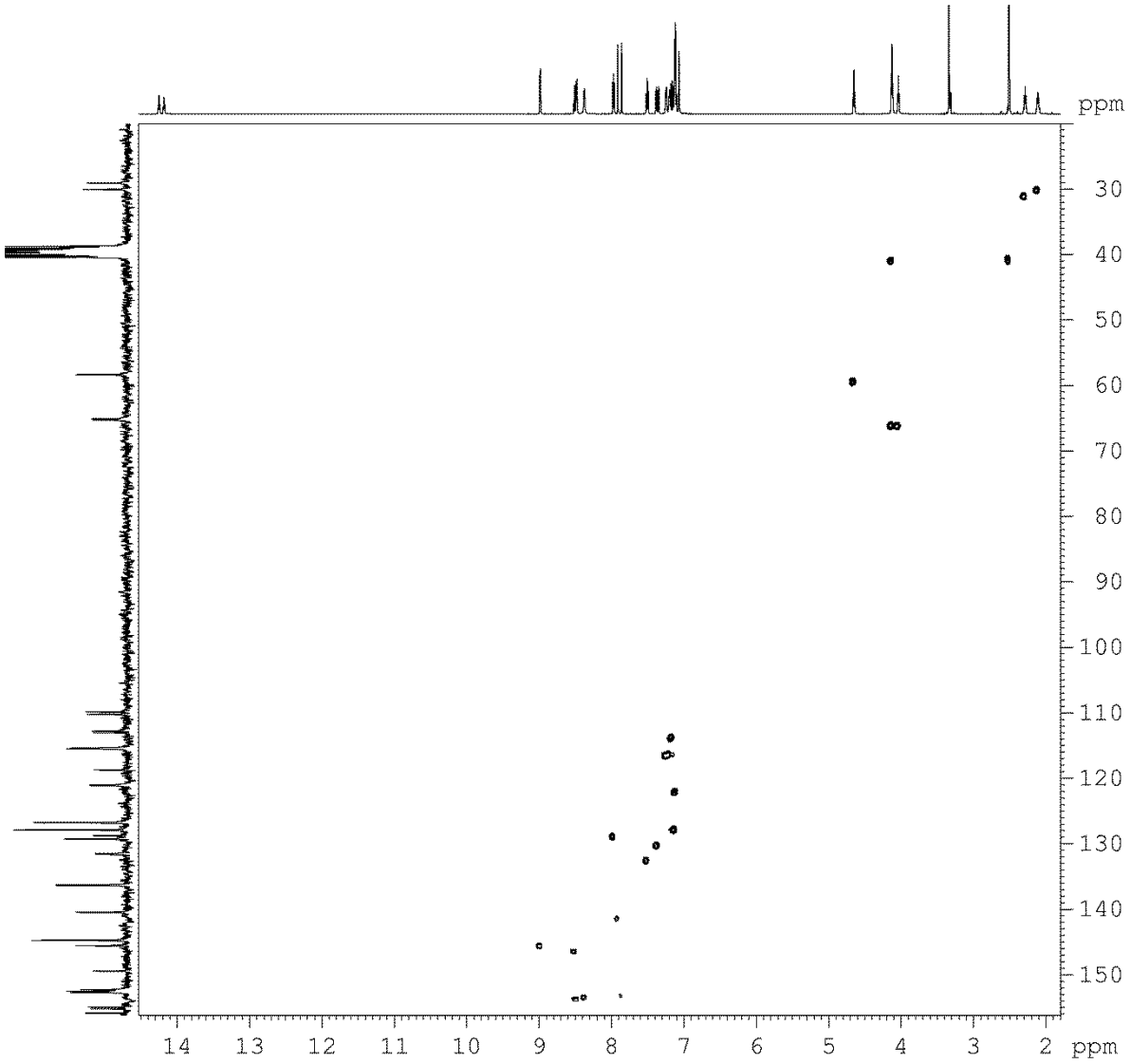

HSQC spectrum of **1**

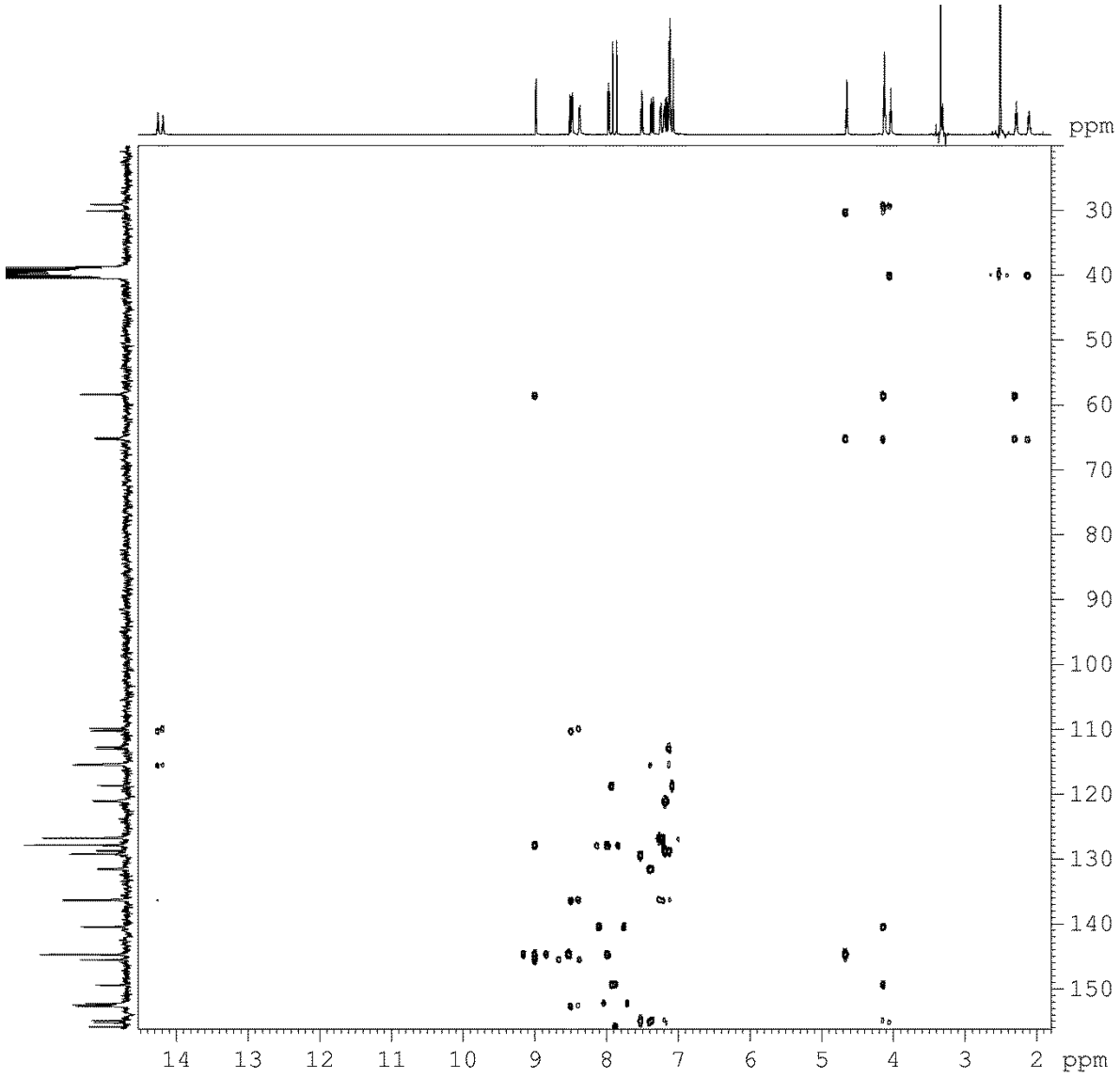

HMBC spectrum of **1**

2 Experimental procedure for Spectroscopy and interactions with DNA/RNA

^{1}H NMR spectra were recorded on Bruker Avance 600 spectrometer (operating at 600.13 MHz for ^{1}H) equipped with TBI probe including z-gradients. Samples in 1 mM sodium cacodylate buffer with 10% D_2O/H_2O were measured at 298 K. Water suppression was achieved using watergate W5 pulse sequence with gradients (from Bruker pulse sequence library). The methyl proton signal of sodium cacodylate buffer was used as internal standard. Proton spectra with spectral width of 12,000 Hz and a digital resolution of 1.4 Hz per point were measured with 128 scans.

Viscometry measurements were conducted with an Ubbelohde viscometer system AVS 370 (Schott). The temperature was maintained at 25 +/- 0.1 °C. Aliquots of drug stock solutions were added to 3.0 ml of 5×10^{-4}mol dm^{-3}ct-DNA solution in sodium cacodylate buffer, I = 0.05 mol dm^{-3}, pH 7.0, with a compound to DNA phosphate ratio r less than 0.2. Dilution never exceeded 4% and was corrected for in the calculations. The flow times were measured at least five times optically with a deviation of ± 0.2 s. The viscosity index α was obtained from the flow times at varying r according to the following equation:[1]

$$L/L_0 = [\,(t_r - t_0)\,/\,(t_{polynucleotide} - t_0)\,]^{1/3} = 1 + \alpha * r$$

Where t_0, $t_{polynucleotide}$ and t_r denote the flow times of buffer, free polynucleotide and polynucleotide complex at ratio $r_{[compound]\,/\,[polynucleotide]}$, respectively; L/L_0 is the relative DNA/RNA lengthening. The L/L_0 to $r_{[compound]\,/\,[polynucleotide]}$ -plot was fitted to a straight line that gave slope α. The error in α is < 0.1.

3 Spectroscopy and interactions with DNA/RNA

Table S1. Electronic absorption data of **1, 2, 3**.

	λ_{max} / nm	$\varepsilon \times 10^3$ / mmol^{-1} cm^2	λ_{max} / nm	$\varepsilon \times 10^3$ / mmol^{-1} cm^2
1	256	29.6 ± 0.3	346	37.6 ± 0.2
2	258	32.5 ± 0.3	346	42.1 ± 0.3
3	254	17.8 ± 0.6	342	32.0 ± 0.9

[a] Sodium cacodylate buffer, I = 0.05 mol dm^{-3},pH = 7.0.

The values of molar extinction coefficient (ε) increase with the length of the linker between DBTAA unit and nucleobase, which could be attributed to the weakening of the intramolecular aromatic stacking interactions proportional to the length of the linker.

3.1. Thermal denaturation experiments

It is well known that upon heating ds-helices of polynucleotides at well-defined temperature (Tm value) dissociate into two single stranded polynucleotides. Non-covalent binding of small molecules to ds-polynucleotides usually has certain effect on the thermal stability of helices thus giving different Tm values. Difference between Tm value of free polynucleotide and complex with small molecule (ΔTm value) is important factor in characterization of small molecule / ds-polynucleotide interactions.

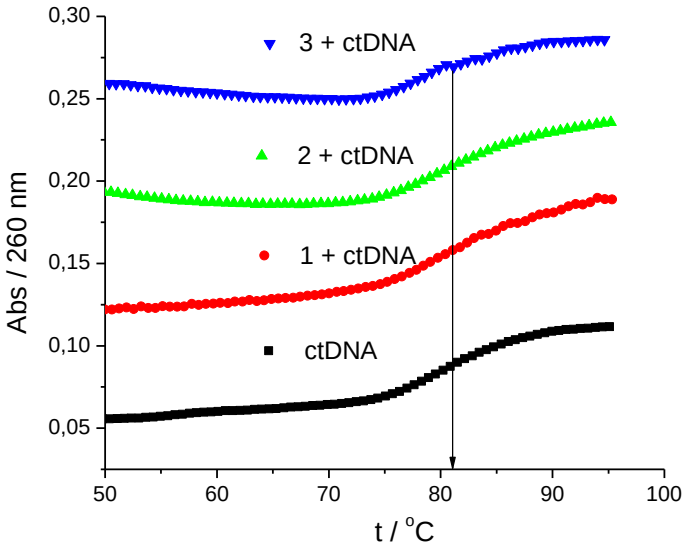

Figure S1. Thermal denaturation curve of **ct-DNA**upon addition of **1** and **2** at $r_{[compound/polynucleotide]}$ = 0.3 and **3** at r = 0.1 (precipitation at higher ratios). Done at pH 7.0 (buffer sodium cacodylate, I = 0.05 mol dm^{-3}).

3.2. Viscometry measurements, CD and gel electrophoresis experiments with ct-DNA

The increase in DNA contour length that accompany an intercalative mode of binding is most conveniently monitored by measuring the viscosity of sonicated rod-like fragments of DNA as a function of ligand binding ratio, r. Cohen and Eisenberg have deduced that the relative increase in contour length in the presence of bound drug is approximated by the cube root of the ratio of the intrinsic viscosity of the DNA-drug complex to that of the free DNA.[1]

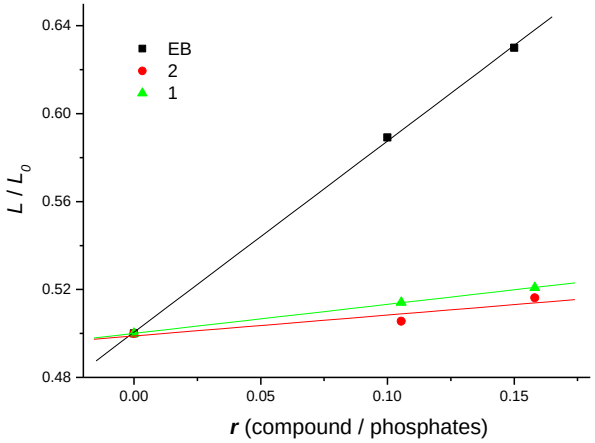

Figure S2. Relative helix length extension of ct-DNA (L/L_0) *vs*. ratio $r_{[compound] / [DNA]}$ plot for **EB**, **1** and **2** at pH 7.0, sodium cacodylate buffer, I = 0.05 mol dm^{-3}.

Viscometry experiments (Figure S2) performed with ct-DNA at pH 7.0 (sodium cacodylate buffer, I = 0.05 mol dm^{-3}) yielded values of α = 0.13 ± 0.01 (**1**), 0.095 ± 0.03 (**2**), and in control experiment for ethidium bromide α(**EB**) = 0.87 ± 0.02. Reference compound **3** precipitated during the experiment.

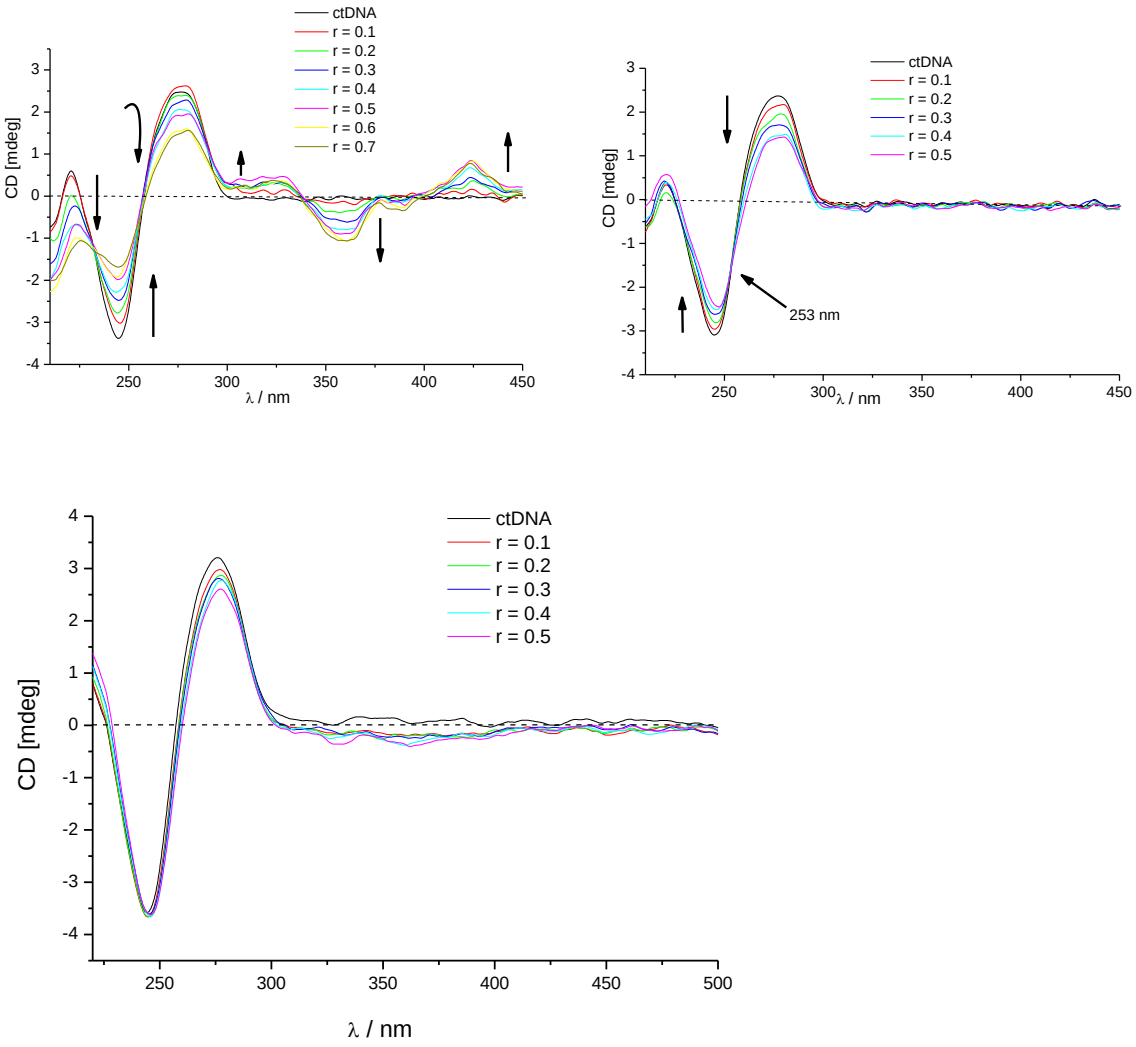

Figure S3. Changes in the CD spectrum of ct-DNA (c = 3.0 × 10^{-5} mol dm^{-3}) upon addition of **1** (left) and **2** (right) and **3** (down) at molar ratios ***r*** = [compound]/ [polynucleotide] (pH 7.0, buffer sodium cacodylate, I = 0.05 mol dm^{-3}).

Agarose gel electrophoresis technique was extensively used for investigating the DNA cleavage efficiency of small molecules and as a useful method to investigate various binding modes of small molecules to supercoiled DNA.[2] Intercalation of small molecules to plasmid DNA can loosen or cleave the SC (*supercoiled*) DNA form, which decreases its mobility rate and can be separately visualized by agarose gel electrophoresis method, whereas simple electrostatic interaction of small molecules to DNA and groove binding does not significantly influence the SC form of plasmid DNA, thus the mobility of supercoiled DNA does not change.[3]

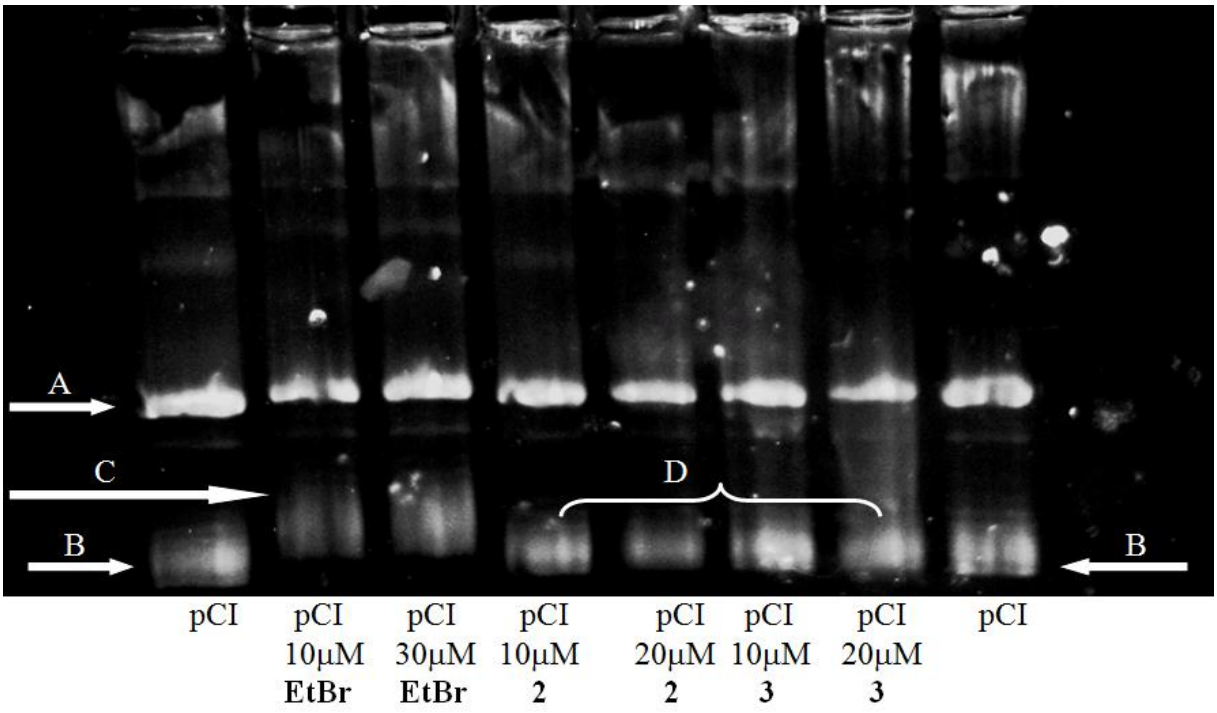

Figure S4. Gel electrophoresis of the supercoiled plasmid DNA, pCI. Arrows point A – open circular plasmid DNA, B – supercoiled circular plasmid DNA, C – supercoiled circular plasmid DNA, retained by intercalated **EB**, D – supercoiled circular plasmid DNA pre-treated with new compounds.

3.3. CD experiments with ss-DNA/RNA

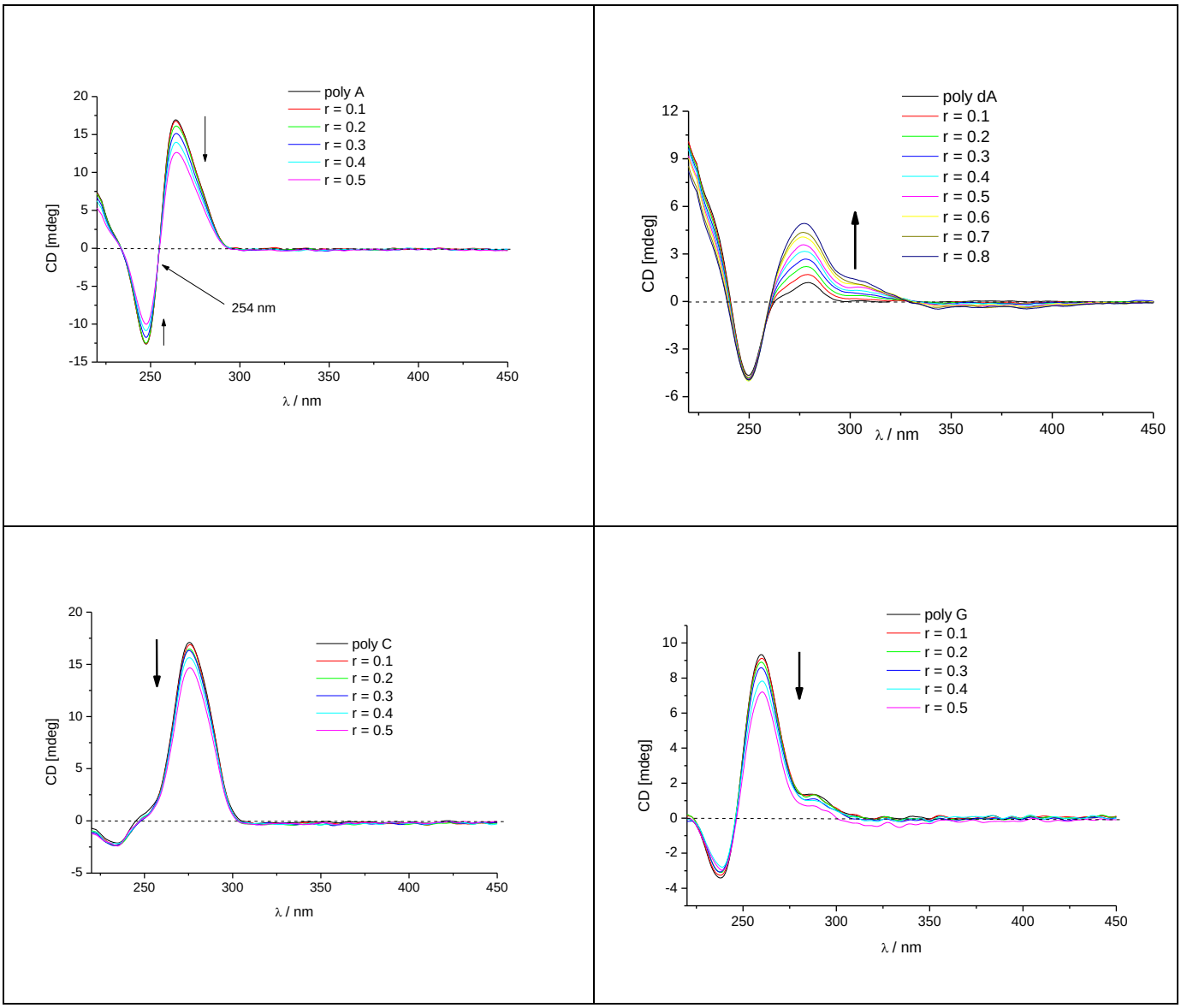

Figure S5. Changes in the CD spectra of ss-polynucleotides (poly A, poly dA, poly C and poly G, c = 3.0 × 10^{-5} mol dm^{-3}), upon addition of **1** at molar ratios ***r*** = [compound]/ [polynucleotide] (pH 7.0, buffer sodium cacodylate, I = 0.05 mol dm^{-3}).

3.4. UV experiments with ss-DNA/RNA

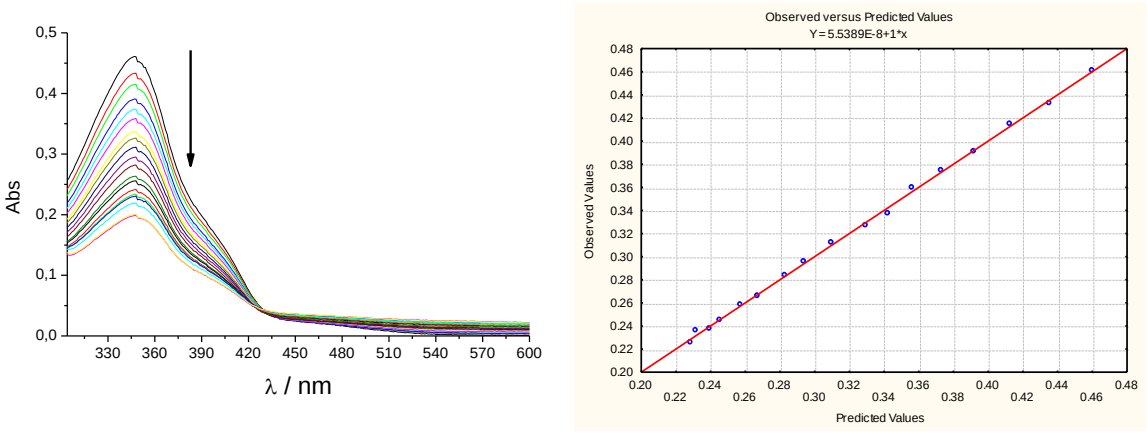

Figure S6. *Left*: Changes in UV/vis spectrum of **1** (c= 1.3 × 10^{-5} mol dm^{-3}) upon titration with poly C (c= 1.7 × 10^{-6} – 1.6 × 10^{-4} mol dm^{-3}); *Right*: Experimental (○) and calculated data (—), processed according to the Scatchard equation, of **1** (λ_{max}=347 nm) as a function of poly C concentration (pH=7, sodium cacodylate buffer, I = 0.05 mol dm^{-3}).

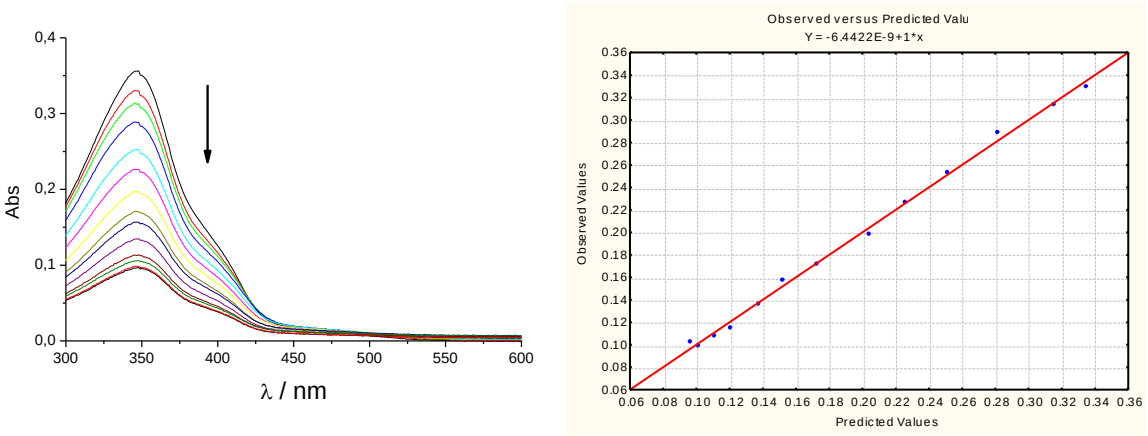

Figure S7. *Left*: Changes in UV/vis spectrum of **1** (c= 1.0 × 10^{-5} mol dm^{-3}) upon titration with poly A (c= 1.9 × 10^{-6} – 1.3 × 10^{-4} mol dm^{-3}); *Right*: Experimental (○) and calculated data (—), processed according to the Scatchard equation, of **1** (λ_{max}=346 nm) as a function of poly A concentration (pH=7, sodium cacodylate buffer, I = 0.05 mol dm^{-3}).

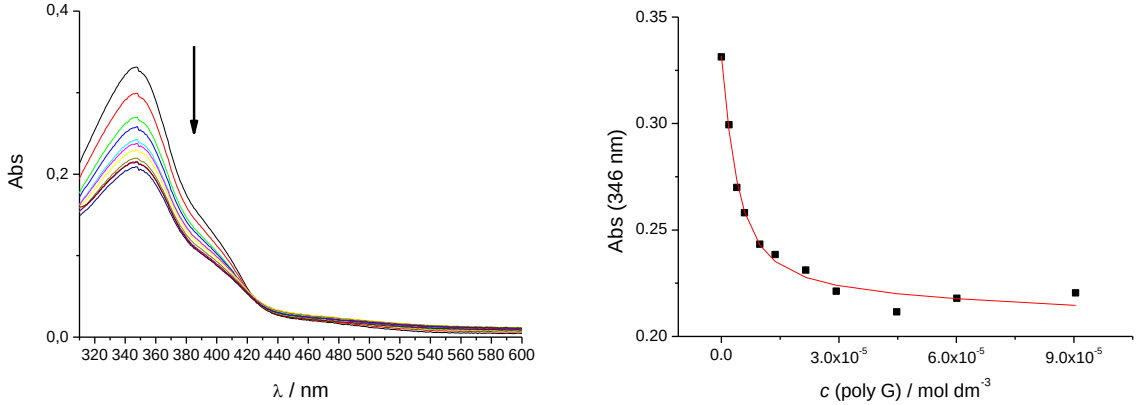

Figure S8. *Left*: Changes in UV/vis spectrum of **1** (c= 1.0 × 10^{-5} mol dm^{-3}) upon titration with poly G (c= 1.9 × 10^{-6} – 9.0 × 10^{-5} mol dm^{-3}); *Right*: Experimental (■) and calculated data (—),

processed according to the Scatchard equation, of **1** (λ_{max}=346 nm) as a function of poly G concentration (pH=7, sodium cacodylate buffer, I = 0.05 mol dm^{-3}).

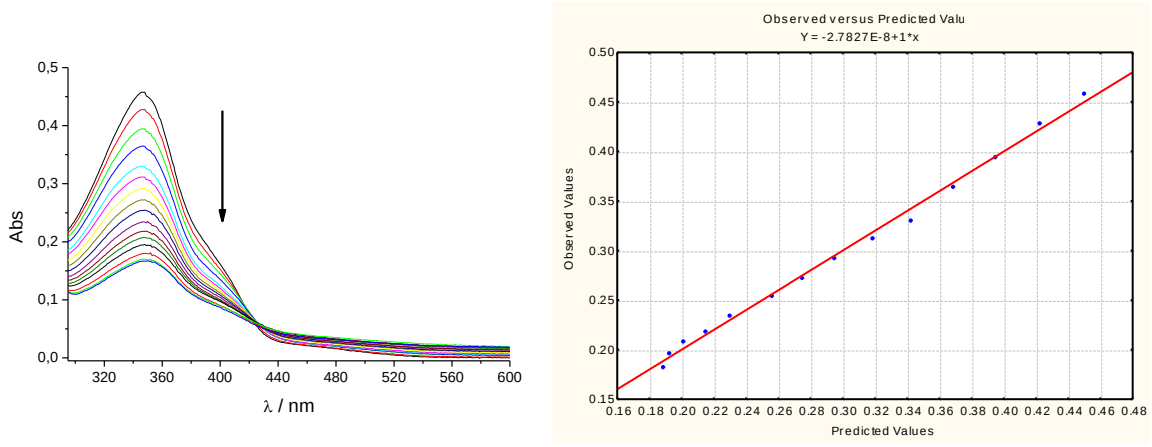

Figure S9. *Left*: Changes in UV/vis spectrum of **1** (c= 1.3 × 10^{-5} mol dm^{-3}) upon titration with poly U (c= 2.8 × 10^{-6} – 1.8 × 10^{-4} mol dm^{-3}); *Right*: Experimental (○) and calculated data (—), processed according to the Scatchard equation, of **1** (λ_{max}=347 nm) as a function of poly U concentration (pH=7, sodium cacodylate buffer, I = 0.05 mol dm^{-3}).

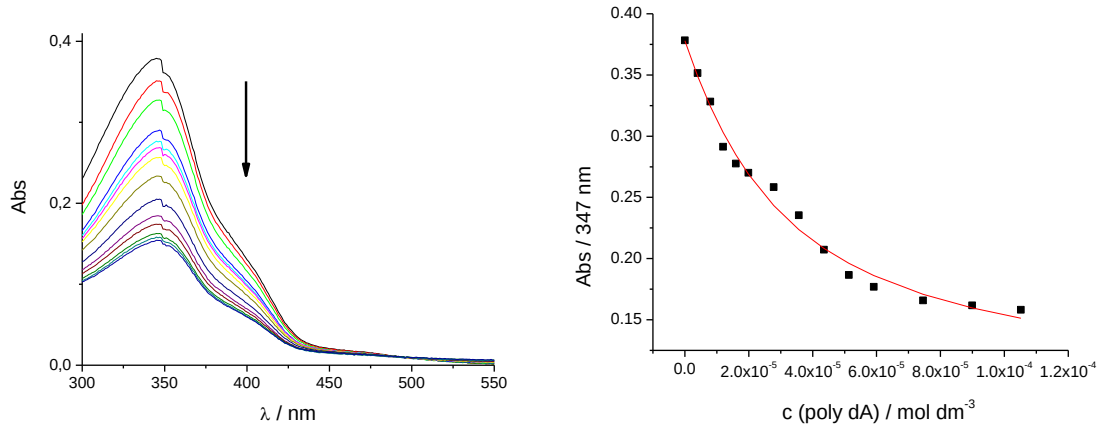

Figure S10. *Left*: Changes in UV/vis spectrum of **1** (c= 9.0 × 10^{-6} mol dm^{-3}) upon titration with poly dA (c= 4.0 × 10^{-6} – 1.0 × 10^{-4} mol dm^{-3}); *Right*: Experimental (■) and calculated data (—), processed according to the Scatchard equation, of **1** (λ_{max}=347 nm) as a function of poly dA concentration (pH=7, sodium cacodylate buffer, I = 0.05 mol dm^{-3}).

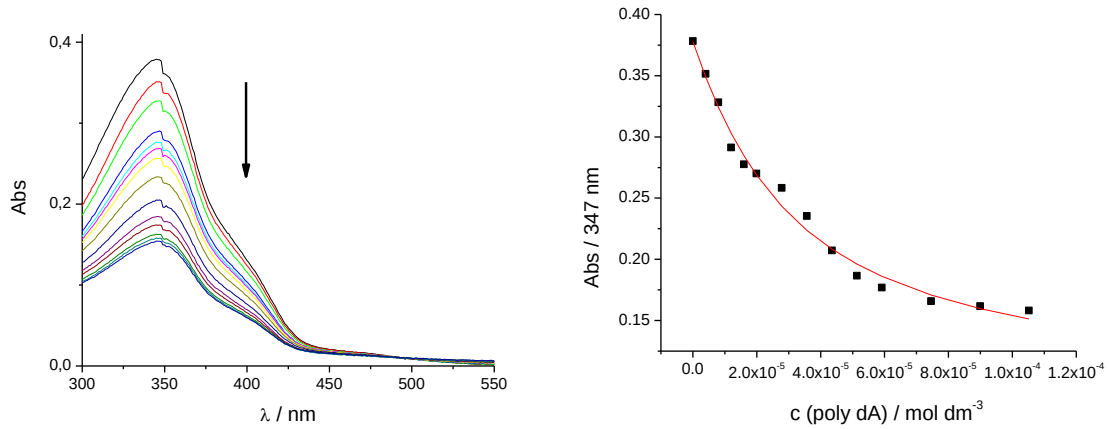

Figure S10. *Left*: Changes in UV/vis spectrum of **1** (c= 9.0 × 10^{-6} mol dm^{-3}) upon titration with poly dA (c= 4.0 × 10^{-6} – 1.0 × 10^{-4} mol dm^{-3}); *Right*: Experimental (■) and calculated data (—), processed according to the Scatchard equation, of **1** (λ_{max}=347 nm) as a function of poly dA concentration (pH=7, sodium cacodylate buffer, I = 0.05 mol dm^{-3}).

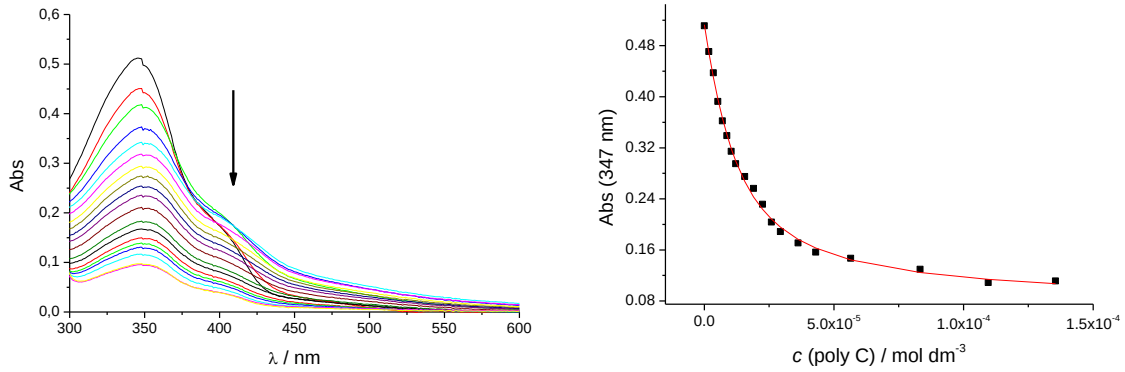

Figure S11. *Left*: Changes in UV/vis spectrum of **2** (c= 1.3 × 10^{-5} mol dm^{-3}) upon titration with poly C (c= 1.7 × 10^{-6} – 1.3 × 10^{-4} mol dm^{-3}); *Right*: Experimental (■) and calculated data (—), processed according to the Scatchard equation, of **2** (λ_{max}=347 nm) as a function of poly C concentration (pH=7, sodium cacodylate buffer, I = 0.05 mol dm^{-3}).

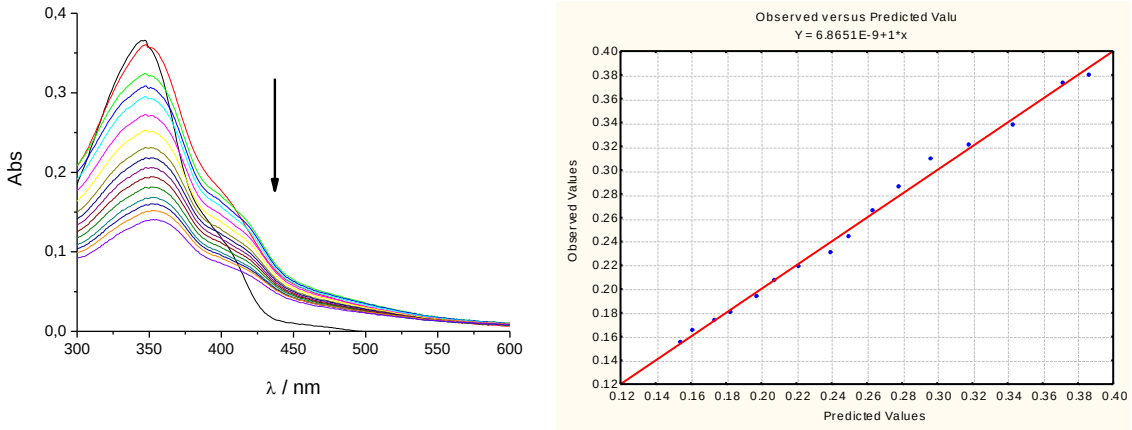

Figure S12. *Left*: Changes in UV/vis spectrum of **2** (c= 8.4 × 10^{-6} mol dm^{-3}) upon titration with poly A (c= 1.9 × 10^{-6} – 1.4 × 10^{-4} mol dm^{-3}); *Right*: Experimental (○) and calculated data (—), processed according to the Scatchard equation, of **2** (λ_{max}=346 nm) as a function of poly A concentration (pH=7, sodium cacodylate buffer, I = 0.05 mol dm^{-3}).

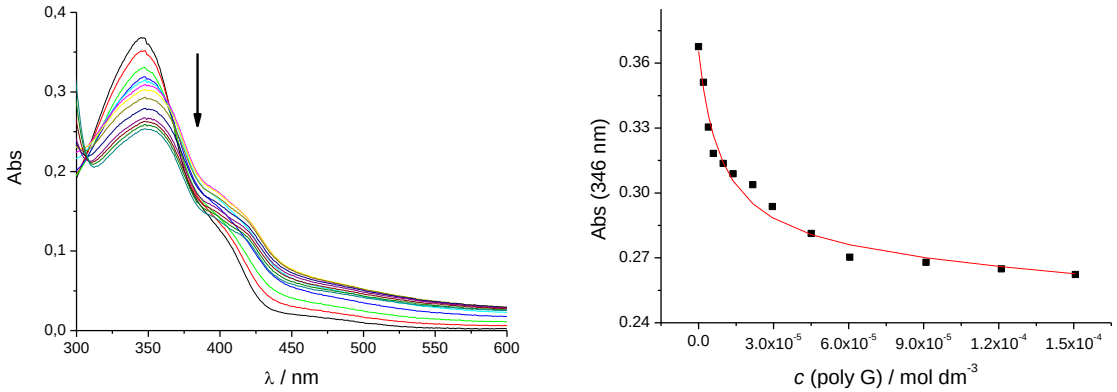

Figure S13. *Left*: Changes in UV/vis spectrum of **2** (c= 9.9 × 10^{-6} mol dm^{-3}) upon titration with poly G (c= 1.9 × 10^{-6} – 1.5 × 10^{-4} mol dm^{-3}); *Right*: Experimental (■) and calculated data (—), processed according to the Scatchard equation, of **2** (λ_{max}=346 nm) as a function of poly G concentration (pH=7, sodium cacodylate buffer, I = 0.05 mol dm^{-3}).

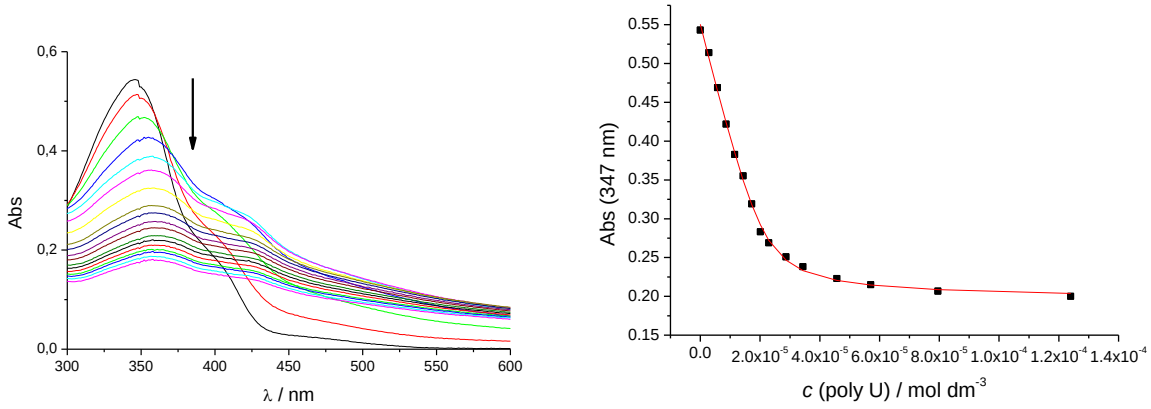

Figure S14. *Left*: Changes in UV/vis spectrum of **2** (c= 1.3 × 10^{-6} mol dm^{-3}) upon titration with poly G (c= 2.9 × 10^{-6} – 2.5 × 10^{-4} mol dm^{-3}); *Right:* Experimental (■) and calculated data (—), processed according to the Scatchard equation, of **2** (λ_{max}=347 nm) as a function of poly G concentration (pH=7, sodium cacodylate buffer, I = 0.05 mol dm^{-3}).

3.5. Competitive CD experiment with poly dT and poly U

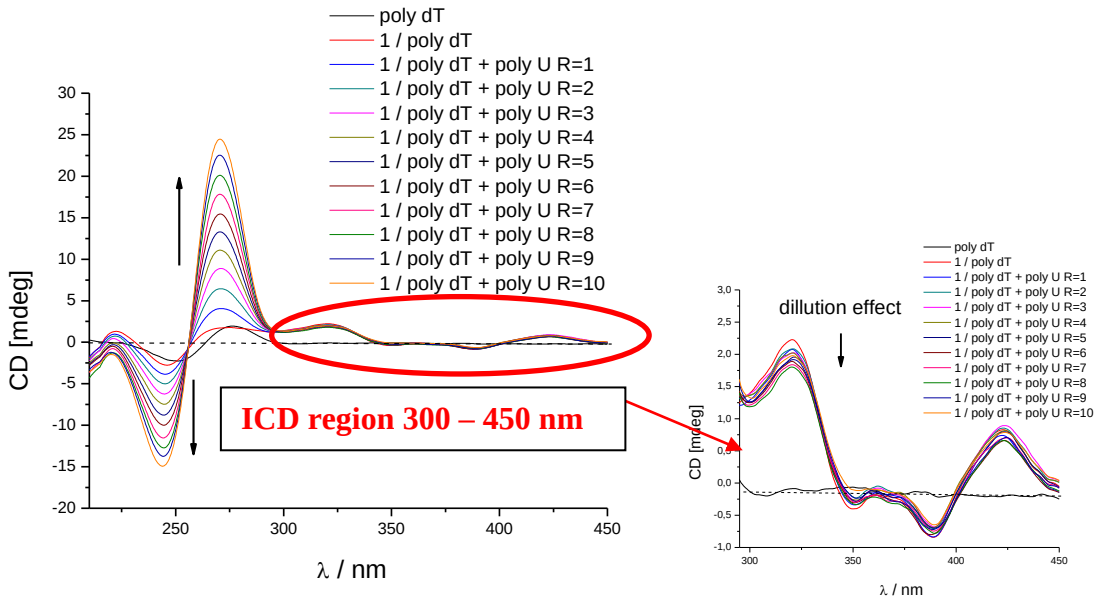

Figure S15. Changes in the CD spectra of **1**/poly dT complex (c(poly dT) = 1.5 × 10^{-5} mol dm^{-3}; c(**1**) = 7.5 × 10^{-6} mol dm^{-3}), upon addition of an 1-10-fold excess of poly U (R= [poly U]/ [poly dT]). Done at pH 7.0, buffer sodium cacodylate, I = 0.05 mol dm^{-3}. **Increase of CD bands at 245 nm and 275 nm corresponds to intrinsic CD spectrum of poly U.**

3.6. UV/vis and CD experiment of 1 with deka dT, titrations with mononucleotides

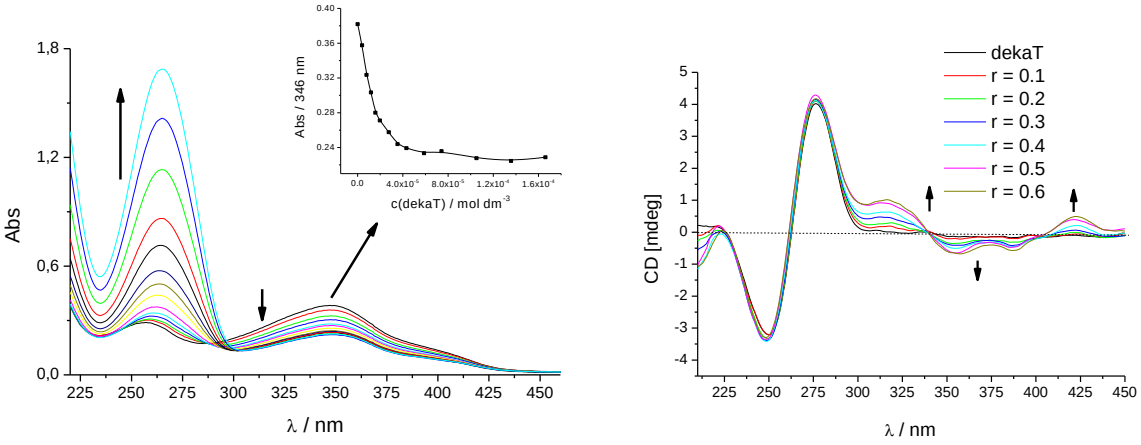

Figure S16a. *Left*: Changes in the UV/vis spectrum of **1** (c = 9.0 × 10^{-6}mol dm^{-3}) upon addition of dekadT. Inset: Dependence of **1** absorbance at λ_{max}= 346 nm on the concentration of dekadT. *Right:* Changes in the CD spectrum of deka dT (c = 3.0 × 10^{-5}mol dm^{-3}) upon addition of **1** at molar ratios ***r*** = [compound]/ [polynucleotide] (pH 7.0, buffer sodium cacodylate, I = 0.05 mol dm^{-3}).

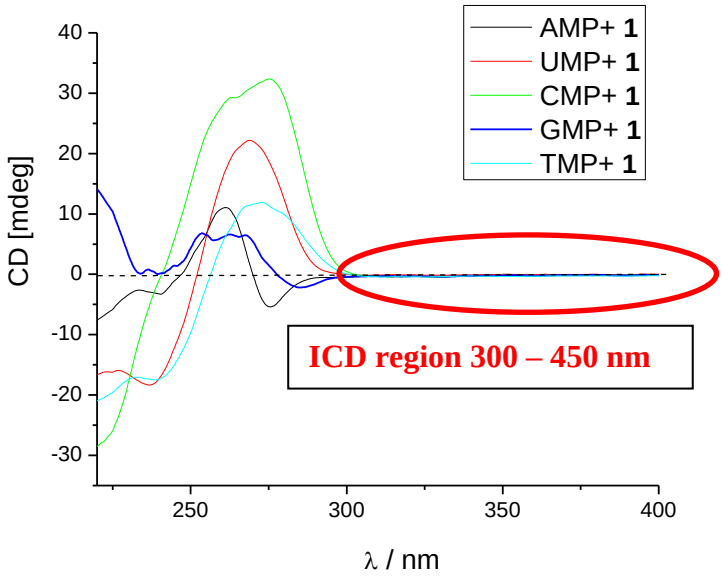

Figure S16b. CD titration of **1** (c= 1.0× 10^{-5} mol dm^{-3}) with AMP, GMP, CMP, UMP and TMP (c= 2.0 × 10^{-4} mol dm^{-3}) at pH 7.0, buffer sodium cacodylate, I = 0.05 mol dm^{-3}.

Table S2. Binding constants (log*Ks*)[a,b] for **1**/nucleotide[d] complexes calculated from the UV/Vis titrations at pH 7.0 (buffer sodium cacodylate, I = 0.05 moldm^{-3})

AMP		GMP		CMP		UMP		TMP	
log*Ks*	[c] H/%	log*Ks*	[c] H/%	log*Ks*	[c] H/%	log*Ks*	[c] H/%	log*Ks*	[c] H/%
4.7	20.9	5.0	21.7	4.9	21.7	4.8	20.2	4.9	23.7

[a]Titration data were processed according to the Scatchard equation; all log*Ks* values were calculated for fixed n=1 (stoichiometry 1 : 1);
[b]Accuracy of $n\pm$ 10 - 30%, consequently log*Ks* values vary in the same order of magnitude;
[c]H=(Abs(**1**) - Abs(complex)) / Abs(**1**)x 100;
[d]AMP = adenosine monophosphate; GMP = guanosine monophosphate; CMP = cytidine monophosphate; UMP = uridine monophosphate; TMP = thymidine monophosphate.

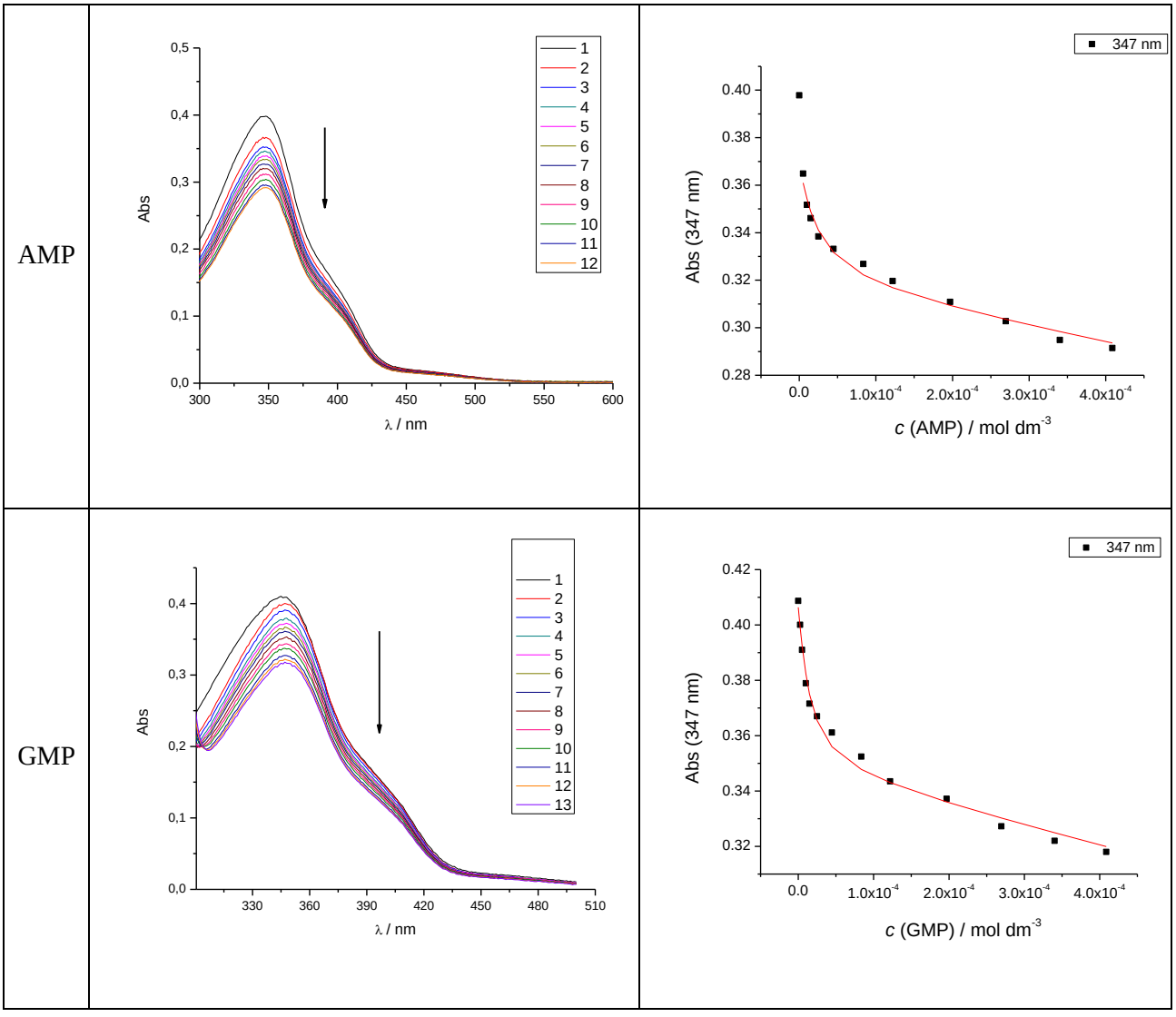

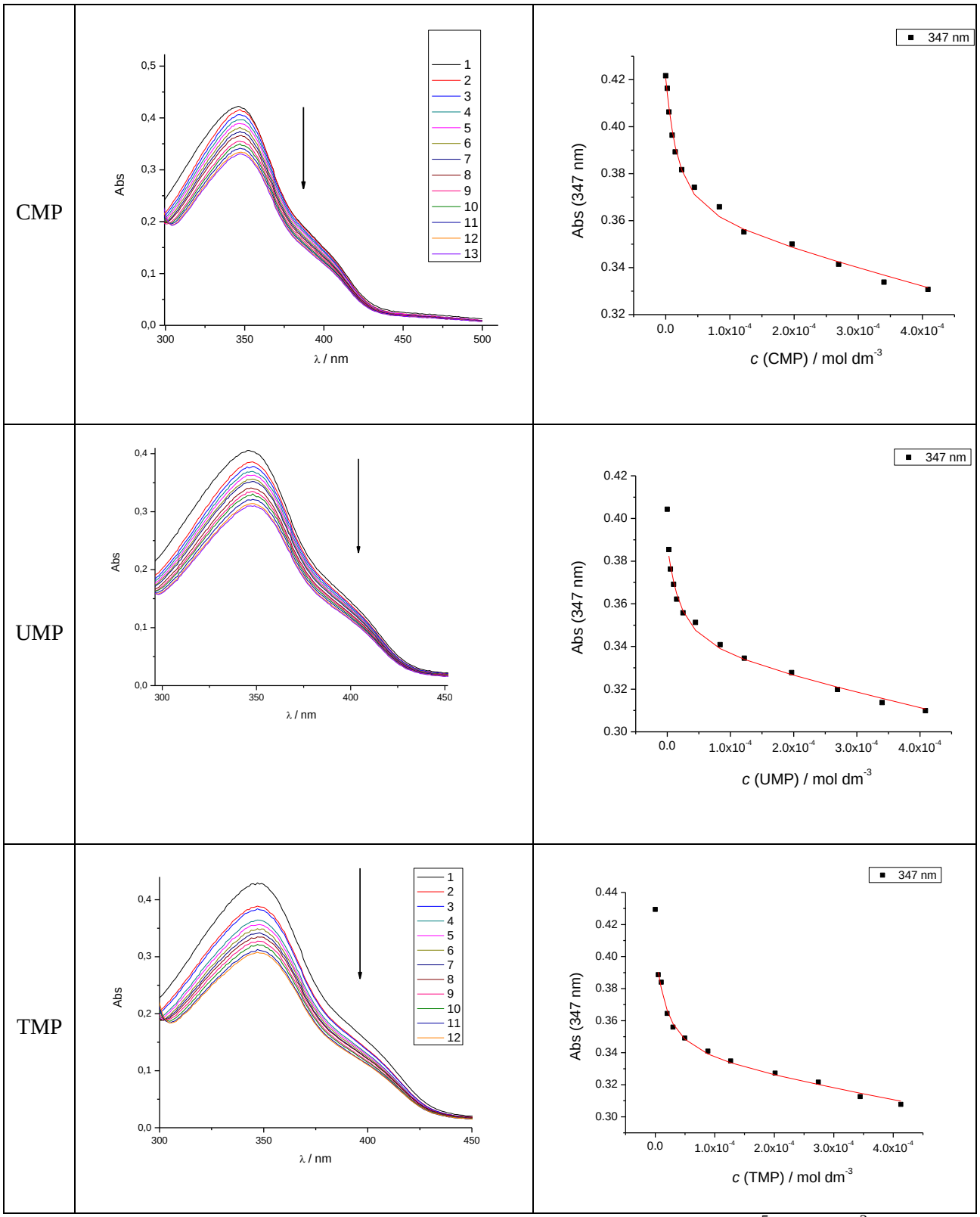

Figure S16c. *left column*) Changes in UV/vis spectrum of **1** (c= 1.0× 10^{-5} mol dm^{-3}) upon titration with AMP, GMP, CMP, UMP and TMP (c= 5× 10^{-6}– 4.0× 10^{-4} mol dm^{-3}); *right column*) Dependence of **1** absorbance at λ_{max} = 347 nm on c(AMP, GMP, CMP, UMP and TMP), at pH=7, sodium cacodylate buffer, I = 0.05 mol dm^{-3}.

4 Molecular modelling: Method and Results

Method

Single stranded tetranucleotides, DNA (poly dT) and RNA (poly rU) were built with the program *nucgen*, a part of the Amber program suit.[4] Compounds **1** and **3** were built using module 'Builder' within program *InsightII*. [5] Complexes with ss-polynucleotides were built by intercalating the aromatic ring of DBTAA into the space between two adjacent bases in the middle of the polynucleotides. The adenine of **1** was oriented in the way form two H-bonds with the polynucleotide-base, (thymine and uracil in the complex with ss-DNA and ss-RNA, respectively).

Parameterization was performed within the AMBER ff99SB force filed of Duan et al.[6] and the general AMBER force field GAFF. Each complex was placed into the center of the octahedral box filled with TIP3 type water molecules, a water buffer of 7 Å was used, and Na^+ ions were added to neutralize the systems. The solvated complexes were geometry optimized using steepest descent and conjugate gradient methods, 2500 steps of each. The optimized complexes were heated in steps of 100 K, each lasting 200 ps, while the volume was kept constant. The equilibrated systems were subjected to 3 ns of the productive unconstrained molecular dynamics (MD) simulation at constant temperature and pressure (300 K, 1 atm) using Periodic Boundary Conditions (PBC). The time step during the simulation was 1 fs and the temperature was kept constant using Langevin dynamics with a collision frequency of 1 ps^{-1}. The electrostatic interactions were calculated by the Particle Mesh Ewald (PME) method with cutoff-distance of 11 Å for the pairwise interactions in the real space. Geometry optimization and molecular dynamics (MD) simulations were accomplished using the AMBER 9 program package.

Results

In the initial complexes between **1** and ss poly-nucleotides (poly dT poly rU)) the substrate was oriented in the similar way with its rings stacked but enabling formation of the hydrogen bonds between adenine and either thymine or uracil (Figures S17 and S18). The complexes were solvated, energy optimized, and subjected to MD simulations. The complex between ss-DNA and **3** was built from the **1**-ss-DNA complex by removing adenine. The initial aromatic stacking between DBTAA and nucleobases of the complexes was not disrupted during the 3 ns of MD simulations at room temperature. However, analysis of the results of MD simulations showed that the complex of **1** with ss-DNA is more stable than the complex with ss-RNA. Besides the aromatic stacking of DBTAA with thymines, one hydrogen bond between adenine and thymine was preserved (green line in Figure 4 in the manuscript), while this was not the case in the complex with ss-RNA (see Figure S18). In Figure S18 on the right side we can see that there are no hydrogen bonds retained between adenine and uracil.

Application of the identical modelling approach to the reference compound **3** revealed a completely different binding mode (Figure S19) whereby **3** does not have adenine to form H-bonds with thymine and in addition the contact of T-methyl with 3-pyridyl is lacking.

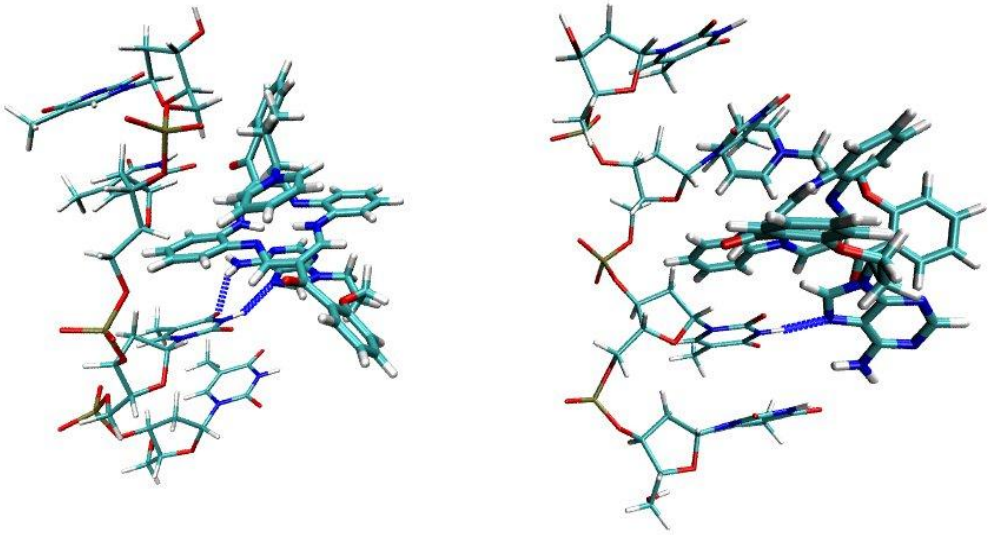

Figure S17: The **1**/poly dT complex: initial optimized (left) and final optimized structure (right).

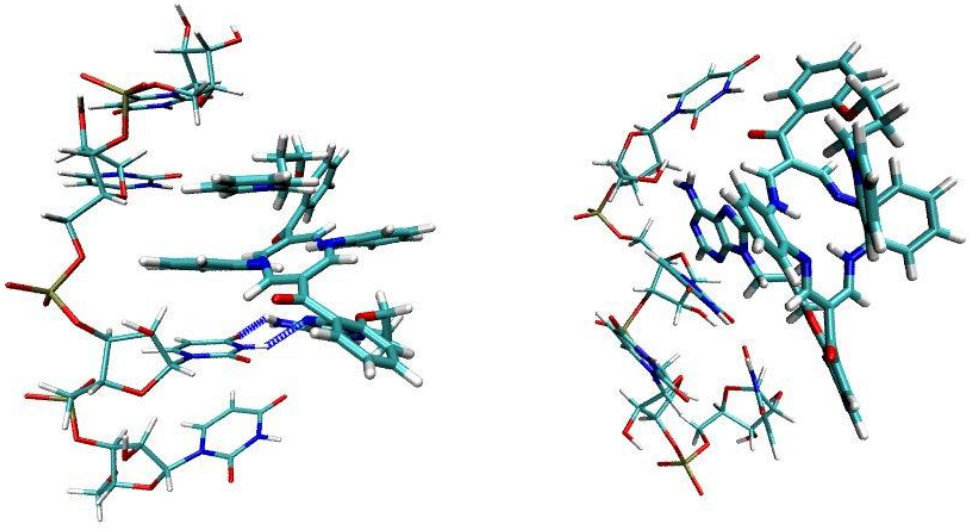

Figure S18: The **1**/poly rU complex: initial optimized (left) and final optimized structure (right).

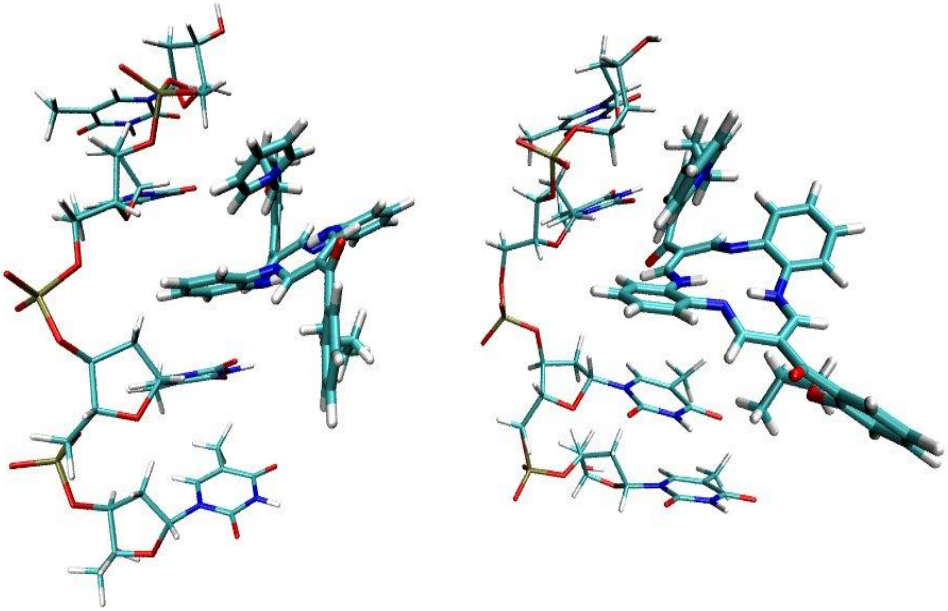

Figure S19: The **3**/poly dT complex: initial optimized (left) and final optimized structure (right).

5. References in Supp. Info.:

1 G. Cohen and H. Eisenberg, *Biopolymers*,1969, **8,** 45; M. Wirth, O. Buchardt, T. Koch, P. E. Nielsen and B. Nordén, *J. Am. Chem. Soc*., 1988, **110,** 932.

2 Y.Li, Z.Yang, *Inorg. Chim. Acta*, 2009, **362**,4823.; C.P. Tan, J. Liu, L –M. Chen, S. Shi, L–N. Ji, *J. Inorg. Biochem.*,, 2008, **102**,1644.; Q. Wang, W. Li, F. Gao, S. Li, J. Ni, Z. Zheng, *Polyhedron*, 2010, **29**, 539.; G. Zuber, J.C. Jr. Quada, S.M. Hecht, *J. Am. Chem. Soc*, 1998, **120**, 9368.

3 Z-F. Chen, L. Mao, L-M. Liu, Y-C Liu, Y. Peng, X. Hong, H-H. Wang, H-G Liu, H. Liang, *J. Inorg. Biochem.*, 2011, **105**,171.

4 http://amber.scripps.edu/

5 INSIGHTII – Accelerys San Diego 2001-2008; http://accelrys.com/services/training/life-science/insight-migration.html

6 Y. Duan, C. Wu, S. Chowdhury, M. C. Lee, G. Xiong. W. Zhang. R. Yang, P. Cipelak, R. Luo and T. Lee, *J. Comput. Chem*., 2003, **24**, 1999.